

Integrating Open-Source Image Processing with Deep Learning for Enhanced Dental Patient Care in Rural Areas

¹Shambhavi M. Shukla, ^{2*}G. R. Mishra

Submitted: 03/02/2024 Revised: 11/03/2024 Accepted: 17/03/2024

Abstract: The objective of this project is to improve dental patient care in remote locations by combining deep learning methods with open-source image processing. A chief radiologist and a team of skilled dentists annotated 196 pairs of periapical radiography pictures that we obtained. The apical areas of teeth were extracted with the application of SIFT and SURF techniques in conjunction with other image preparation procedures. Several image calibration approaches were used in the tooth apical section extraction procedure to enhance feature extraction and matching. For the purpose of classifying dental photos, a convolutional neural network (CNN) was trained using clipped periapical images as inputs. To avoid overfitting, dropout and L2 norm regularization were used. Weight changes were performed using a decreasing learning rate schedule and stochastic gradient descent (SGD). Findings demonstrated higher F1 scores in comparison to baseline techniques, proving the usefulness of the suggested strategy. The work shows how deep learning and image processing might be used to improve dental treatment in remote locations.

Keywords: : Dental care, rural areas, image processing, deep learning, periapical radiography, convolutional neural network..

1. Introduction

Applications in medical imaging research are becoming more and more important as a result of big data availability and artificial intelligence (AI) technology's ongoing advancement [1]. AI has demonstrated significant promise to support dental treatment planning and illness diagnostics [2]. Numerous applications in the area of dentistry have resulted from deep learning models' exceptional capacity to understand complicated patterns from big picture datasets [3]. Dental radiograph deep learning has shown to be an effective and accurate way to identify dental problems. An efficient method for the identification of dental illnesses may be built by utilizing convolutional neural networks. Particularly with regard to common dental conditions like periodontitis and dental caries, oral illness is a significant global public health concern. A chronic inflammatory illness of the gums and teeth, periodontitis is typified by the breakdown of alveolar bone and the surrounding tissues, particularly the periodontal ligament. Dental plaque is the primary cause of periodontitis, causing a cascade of inflammatory responses and the breakdown of periodontal tissues. Research has shown that periodontitis may be linked to other significant systemic disorders or raise the risk of cardiovascular disease [4]. Dental caries is a condition mostly brought on by acid erosion that can harm tooth structure. The intraoral microbes are the

essential makers of the corrosive. The two most normal oral diseases that lower personal satisfaction are periodontitis and dental caries [5]. Two of the most well-known oral diseases on the planet that influence a sizable segment of the populace are periodontitis and dental caries [6,7,8]. The general condition of wellbeing and oral wellbeing can be fundamentally affected by these two circumstances. As a result, one of the most crucial jobs for dentists is to prevent dental cavities and periodontitis. Moreover, treating periodontitis and tooth cavities has historically depended heavily on early detection. Clinical and radiographic exams are the primary means of detecting dental caries and periodontitis. In order to give a thorough diagnosis and treatment plan, dentists usually assess a number of different areas of a patient's oral health. The simultaneous detection of dental caries and periodontitis using AI-assisted technology is akin to the way dentists diagnose patients in clinical settings [9]. It is possible to minimize patient discomfort from repeated examinations, save time for dentists, and lessen their workload.

1. Literature Review

Deep learning methods may be applied as they aid in the identification, extraction, and creation of new highlights. Artificial intelligence (AI) is defined as a collection of devices that can recognize patterns in data and then use those patterns to forecast and assist in dynamic tasks.[10] Artificial intelligence (AI) and machine learning techniques can be used in various clinical domains, such as clinical image handling, clinical image translation, clinical image division, clinical image combination, clinical image enrollment, clinical image recovery, and clinical image guided treatment. These techniques can also effectively, precisely, and proficiently extract and communicate with

^{1,2}Dept of Physics and Electronics Dr Rammanohar Lohia Avadh University, Ayodhya

Corresponding Mail : grmishra@gmail.com

data from images. These techniques aid experts in more accurate and timely analysis and prediction of disease risk. It motivates them to investigate the non-exclusive alterations that may cause illness. These procedures incorporate the accompanying: profound Boltzmann machine, profound conviction organization, profound auto encoder, long transient memory, profound brain organization, profound traditional, outrageous learning machine, generative badly arranged frameworks, etc [11]. Deep learning may be defined as a special type of artificial neural network that mimics the dynamic process of human beings in some ways. [12] It is receiving a lot of attention because of its use in vast amounts of social insurance data. The first fake neural system was introduced in the middle of the 1950s, but due to its flaws—such as overfitting, vanishing slope, and other issues—the engineering process was slowed down. Additionally, at that time, there wasn't enough knowledge or computing power to prepare the framework.

1. Methodology

Our study's goal was to enhance dental patient care in rural locations by combining deep learning methods with open-source image processing.

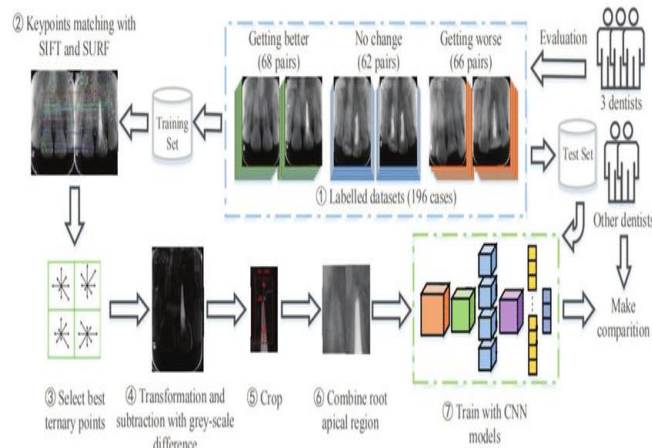


Figure 1: Automated Analysis of Dental Images for Clinical Outcome Evaluation

Figure 1 describes the approach we took to accomplish this. Getting an experimental dataset with 196 pairs of periapical radiography pictures was the initial step. Before and after therapy, these pictures were captured. Three qualified dentists and a top radiologist made up our expert team that classified the dataset to guarantee its quality and dependability. This dataset provided the essential input for our later image processing and deep learning investigations, which formed the basis of our study. Because of our team's experience, the dataset was extensive and representative of actual dental situations, which increased the applicability and relevance of our study's findings for enhancing dental treatment in rural

regions [13]. We used a sequence of picture preprocessing techniques in order to extract the regions of interest (ROIs), more precisely the apical areas. First, we identified feature points between the picture pairings using the Scale-Invariant Feature Transform (SIFT) and Speeded-Up Robust Features (SURF) techniques. Afterwards, we employed the least greyscale difference approach to identify the optimal ternary matching locations. These locations served as the basis for our calculation of the affine matrix, which we then used to perform image subtraction and highlight the canal filling areas in order to pinpoint the root region. After that, the apical section of the root was chopped and two channels of the pre-treatment picture were combined.

A. Tooth apical portion extraction

We faced difficulties in extracting the apical region of the tooth since there wasn't enough labeled data. Results were not good enough when original photos were used to train the classification network directly. In order to enhance the training procedure, we thus made the decision to further analyze the input photos, paying particular attention on locating the apical area of the infected root canal. We used a number of image calibration approaches to improve the photos for more accurate feature extraction and matching. First, we performed feature matching using the SIFT and SURF methods.

Feature Matching Score Calculation (for SIFT and SURF):

$$Score(p_1, p_2) = \sum w_i \times Distance(fi^{(1)} fi^{(2)}) \dots\dots (3.1)$$

Where p_1 and p_2 are the keypoints, $fi^{(1)}$ and $fi^{(2)}$ are the feature descriptors, w_i are the weights, and Distance is the distance metric (e.g., Euclidean distance)

Because of their adaptability to changes in scale and direction, these algorithms are often employed and are appropriate for our objective. To further emphasize important areas in the photos, we used unsharp masking techniques and histogram equalization. By enhancing the contrast of the photographs, histogram equalization aids in highlighting and highlighting the characteristics for easy identification. On the other hand, unsharp masking sharpens the edges and details in the photos, enhancing the quality of the main points even more. Lastly, we automated picture calibration using affine transformation. We were able to adjust for variations in translation, rotation, and scale between the photos taken before and after the therapy using this method. We were able to precisely remove the pictures to highlight the filling regions—which are essential for determining the tooth's apical region—by aligning the images using affine transformation Equation:.

$$\begin{bmatrix} x \\ y \\ 1 \end{bmatrix} = \begin{bmatrix} a & b & tx \\ c & d & ty \\ 0 & 0 & 1 \end{bmatrix} \begin{bmatrix} x \\ y \\ 1 \end{bmatrix}$$

where (x,y) are the changed directions, (x,y) are the first arranges, and a,b,c,d,tx,ty are the components of the relative change network.

A. Dental Image Classification Model

We used a convolutional neural network (CNN) structure, which is well-suited for image processing applications, to create our dental image categorization model. The preprocessed, cropped photos of the periapical areas were the network's inputs. The photos were acquired by following a sequence of procedures defined previously in the research. We integrated the pre- and post-treatment photos into two channels to provide the network information from both sets of images. This made it possible for the network to examine the variations in the photos, which is essential for assessing the treatment's clinical quality. We implemented dropout in between the fully connected layers to avoid overfitting, a problem that frequently arises in deep learning models. During training, dropout randomly eliminates a percentage of the network's neurons, which helps the network become less dependent on any one parameter and enhances its capacity for generalization. Furthermore, we modified the loss function to include L2 norm regularization.

Loss Function with L2 Regularization:

$$Loss = CrossEntropyLoss + \lambda \left(\sum_{i=1}^N w_i^2 \right)$$

Where

CrossEntropyLoss is the standard cross-entropy loss, λ is the regularization parameter, N is the total number of weights in the network, and w_i are the weights.

Large weights in the network are penalized by L2 norm regularization, which might assist avoid over fitting by pushing the network to find easier patterns in the data. To update the network's weights, we employed stochastic gradient descent (SGD) rule:

$$w_{t+1} = w_t - \eta \Delta Loss$$

Where w_{t+1} is the refreshed weight, w_t is the ongoing weight, η is the learning rate, and $\nabla Loss$ is the angle of the misfortune capability regarding the weight.

SGD is a well-known profound learning enhancement method that changes the loads as per the slope of the misfortune capability with respect to the loads. To aid in the model's convergence to a better solution, we also used a declining learning rate schedule, in which the learning rate was gradually lowered.

$$\eta_t = \eta_0 \times decay^{\left(\frac{t}{step}\right)}$$

Where η_t is the learning rate at iteration t, η_0 is the initial learning rate, decay is the decay rate, and step is the number of iterations after which the learning rate is decayed.

With the momentum parameter set to 0.9, SGD is accelerated in the appropriate directions and oscillations are dampened.

A. Datasets

Initial, a dataset of 196 sets of periapical dental radiographs was recognized and explained. Every radiograph goes on the defensive toward are under treated; each pair incorporates radiographs taken when the technique. In view of clinical perception, gifted dental specialists characterized these teeth as "improving," "no change," or "deteriorating." A normalized procedure was utilized to take the radiographs, which incorporated an openness time of 0.20 seconds, a cylinder voltage of 70 KV, and a cylinder current of 6 Mama.

During the examination, radiologists could make a few minor modifications to these parameters. Because the radiographs were obtained with the bisecting angle technique, each tooth had a different shooting angle. We used data augmentation to enhance the dataset by rotating the photos gradually, flipping them horizontally and vertically, and varying the brightness of the images within a predetermined range to replicate various real-world examination settings.

2. Results

A. Automated Calibration and Cropping of Apical Region

Initially, the input photos we utilized contained the complete tooth. However, we ran across issues like dental wear and neighbouring teeth overlap on X-rays, which made the issue noisier. We made the decision to decrease the size of the input photos in order to solve these problems and prevent over fitting brought on by the dataset's small sample instances. In light of dentists' experience, we concentrated on removing the tooth's apical part for examination.

```

clc;
clear all;
close all;

image_name='10.gif.jpg'; %%Change this if you ha

teeth_image=imread(image_name);
subplot(1,2,1)
imshow(teeth_image)
grayscale_teeth=rgb2gray(teeth_image);

segmented_teeth=im2bw(grayscale_teeth,0.4);
subplot(1,2,2)
imshow(segmented_teeth);

```

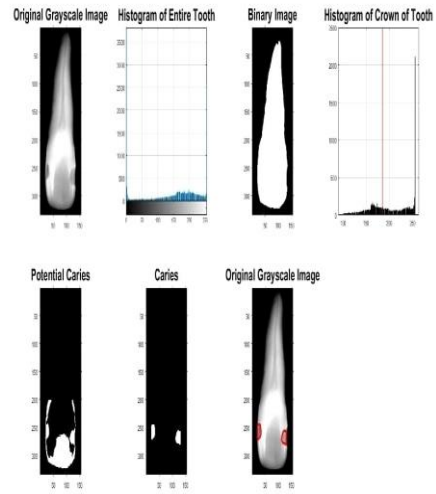


Fig.4 Analysis Of teeth Segment By using Deep Learning.

Table 1: Result of automated calibration and cropping.

Classes	Front teeth		Molars	
	Calibration	Crop	Calibration	Crop
Improving (68)	52/58	50/65	15/32	8/15
No change (62)	36/45	30/40	26/35	16/35
Deteriorating (66)	32/40	25,40	15/36	9/36

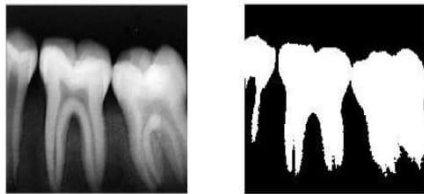


Fig.1 Result Of Automated X-Ray Analysis

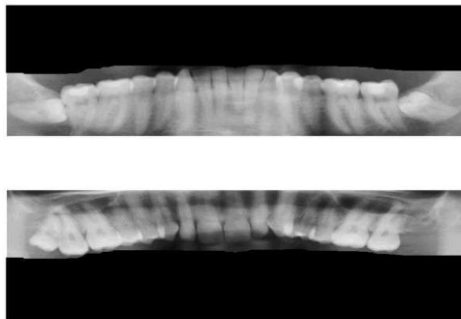


Fig.2 Result of automated calibration and cropping Analysis

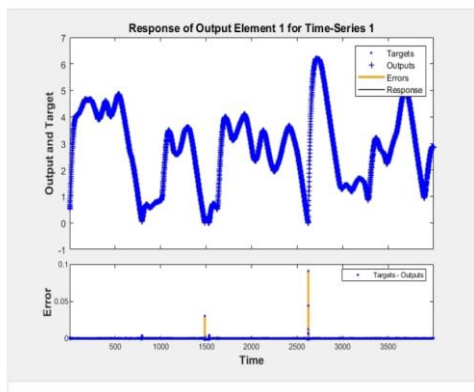


Fig.3 Response Of Output Element.

We employ the procedure for automatic apical area cropping and calibration across the board in the dataset. Our approach outperforms the current approach. [14] amid hazy circumstances.

Table I demonstrates that the automated calibration approach used in this article produces good results on the majority of dental photos, particularly those showing the front teeth. Additionally, once properly calibrated, there will be a greater possibility of obtaining an optimal crop result for photographs of the front teeth. On molar pictures, however, our strategy is not always effective. Some picture disparities are so great that manual calibration is not even effective when based just on the affine matrix. As a result, in the future, we must investigate fresh approaches to handle these picture pairings.

B. Classification Network

We tested a number of network topologies to automatically crop the dataset with the apical section. Although it converges at a somewhat slower rate than AlexNet—10,000 iterations—it achieves a greater level of accuracy. Furthermore, GoogLeNet, a more profound organization, doesn't merge on our dataset. While a more profound organization design will bring about over-fitting C, the proposed network delivers the best trial results.

C. Assessment of Clinical Outcomes

- **Baseline:**

We contrast our method with baseline techniques for classifying images (Table 2). These baseline techniques all make use of a classifier and feature extraction. Images of the manually clipped root apical area are used to extract features. Subsequent to removing the picture highlights utilizing the Histogram of Oriented Gradients (HOG), Principal Components Analysis (PCA), Greyscale Histogram, and subsampling method, we group the pictures utilizing Support Vector Machine (SVM), k-nearest neighbors (KNN), Gradient Boosting Decision Tree (GBDT), Random Forest (RF), Naive Bayes (NB), and AdaBoost. To display the best F1 score for each algorithm, we adjusted the settings of the features and the classifiers. Classifiers such as GBDT and AdaBoost obtain greater scores, as Table II illustrates. Furthermore, the greatest F1 score of 0.650 is obtained by applying GBDT and analyzing HOG features using PCA.

Table 2: Result of F1 scores in baseline method

Method	Histogram	Subsampled	HOG	PCA	HOG+PCA
SVM	.423	.523	.485	.512	.645
KNN	.363	.545	.475	.336	.551
GBDT	.412	.623	.476	.612	.645
RF	.485	.640	.485	.523	.520
NB	.363	.512	.441	.345	.596
AdaBoost	.485	.663	.512	.412	.523

- **Our approach:**

The typical F1 scores of a few tests utilizing the entire tooth and the apical locales of the root as data sources are shown in Table 3. It is apparent that utilizing the root apical region instead of the entire tooth further develops F1 scores. We explore different avenues regarding two methodologies for blending pre-and post-treatment pictures: putting them one next to the other in one channel and coordinating them into two channels. The latter is shown to perform better and can also minimize parameters. The examples in the "Deteriorating" group did not yield as excellent of outcomes as those in the "Improving" category. Next, we sent an invitation to one chief radiologist and two dental specialists to take part in the comparative analysis. The test dataset was labeled independently by each dentist. We see that various dentist outcomes clearly differ from one another. Comparable to our network, the average dentist's findings show that the "Improving" cases have the greatest F1 score, while the "Deteriorating" cases have the lowest. Additionally, in circumstances when the tooth is "getting better," dentists can make judgments throughout the labeling process more swiftly. On the other hand, "no change" and "

Deteriorating" are less evident. The confusion matrix further illustrates this point: while both our suggested network and the dentists are more accurate in the "Improving" situations, they are more prone to making mistakes in the "Deteriorating" ones. Table 3 shows that our network's F1 score is greater than the average of the dentists' performance across the three classes, indicating that our automated assessment streamlining technique outperforms experts in this domain.

Table 3: F1 Scores of Different Methods for Quality Evaluation

Method	the Man	Aut	Aut	dent	dent	dent	
	wh	ual	o	io	ist	ist	
	ole	crop	cro	cro	1	2	
	toot	p+	p*			3	
	h						
Class level	Improvi	0.4	0.84	50.7	0.7	0.74	0.66
	ng	12	45	45	5	5	2
F1 Score	No	0.5	0.74	50.7	0.7	0.45	0.70
	change	23	15	55	2	5	5
	Deterior	0.4	0.71	20.7	0.7	0.17	0.84
	ating	11	03	11	4	5	2
Aggregate Result	Precisio	0.5	0.75	80.7	0.7	0.65	0.87
	n	12	45	56	6	8	5
	Recall	0.4	0.74	70.7	0.7	0.41	0.74
	s	85	21	14	2	5	9
	F1	0.5	0.77	10.7	0.7	0.55	0.80
		23	36	41	2	3	4

3. Conclusion

The study demonstrates the effectiveness of integrating open-source image processing with deep learning techniques to improve dental patient care in rural areas. By employing a series of image processing steps, including feature matching, histogram equalization, unsharp masking, and affine transformation, we were able to accurately extract the tooth apical portion from periapical radiography images. Additionally, our dental image classification model, based on a convolutional neural network structure, showed promising results in evaluating clinical outcomes. The model's ability to analyze pre- and post-treatment images and classify them based on clinical quality provides a valuable tool for dentists in assessing treatment effectiveness. Overall, our study highlights the potential of combining advanced image processing and deep learning methods to enhance dental care practices, particularly in underserved rural areas.

REFERENCES

[1] A.S. Panayides et al., "AI in medical imaging informatics: Current challenges and future

- directions," *IEEE J. Biomed. Health Inform.*, vol. 24, pp. 1837–1857, 2020, doi: 10.1109/JBHI.2020.2991043.
- [2] T. Kishimoto et al., "Application of artificial intelligence in the dental field: A literature review," *J. Prosthodont. Res.*, vol. 66, pp. 19–28, 2022, doi: 10.2186/jpr.JPR_D_20_00139.
- [3] Y. Suhail et al., "Machine learning for the diagnosis of orthodontic extractions: A computational analysis using ensemble learning," *Bioengineering*, vol. 7, p. 55, 2020, doi: 10.3390/bioengineering7020055.
- [4] F. Schwendicke et al., "Convolutional neural networks for dental image diagnostics: A scoping review," *J. Dent.*, vol. 91, p. 103226, 2019, doi: 10.1016/j.jdent.2019.103226.
- [5] R.S. Rao et al., "Ensemble deep-learning-based prognostic and prediction for recurrence of sporadic odontogenic keratocysts on hematoxylin and eosin stained pathological images of incisional biopsies," *J. Pers. Med.*, vol. 12, p. 1220, 2022, doi: 10.3390/jpm12081220.
- [6] A. Falcão and P. Bullón, "A review of the influence of periodontal treatment in systemic diseases," *Periodontol. 2000*, vol. 79, pp. 117–128, 2019, doi: 10.1111/prd.12249.
- [7] R.G. Watt et al., "London charter on oral health inequalities," *J. Dent. Res.*, vol. 95, pp. 245–247, 2016, doi: 10.1177/0022034515622198.
- [8] J.H. Lee et al., "Diagnosis and prediction of periodontally compromised teeth using a deep learning-based convolutional neural network algorithm," *J. Periodontal Implant Sci.*, vol. 48, pp. 114–123, 2018, doi: 10.5051/jpis.2018.48.2.114.
- [9] H. Li et al., "An interpretable computer-aided diagnosis method for periodontitis from panoramic radiographs," *Front. Physiol.*, vol. 12, p. 655556, 2021, doi: 10.3389/fphys.2021.655556.
- [10] H. Ehtesham et al., "Developing a new intelligent system for the diagnosis of oral medicine with case-based reasoning approach," *Oral Dis.*, vol. 25, no. 6, pp. 1555–1563, 2019.
- [11] E.J. Topol, "High-performance medicine: the convergence of human and artificial intelligence," *Nat. Med.*, vol. 25, pp. 44–56, 2019.
- [12] T. Hiraiwa et al., "A deep-learning artificial intelligence system for assessment of root morphology of the mandibular first molar in panoramic radiography," *Dentomaxillofac Radiol.*, vol. 48, no. 3, p. 20180218, 2019.
- [13] Y.C. Chen et al., "Improving dental implant outcomes: CNN-based system accurately measures degree of peri-implantitis damage on periapical film," *Bioengineering*, vol. 10, p. 640, 2023, doi: 10.3390/bioengineering10060640.
- [14] H. Chen and A.K. Jain, "Tooth contour extraction for matching dental radiographs," in *Pattern Recognition, 2004. ICPR 2004. Proceedings of the 17th International Conference on*, vol. 3, IEEE, 2004, pp. 522–525.
- [15] M. Khan et al., "Dental Image Analysis Approach Integrates Dental Image Diagnosis," *Int. J. Curr. Res. Rev.*, vol. 12, pp. 47–52, 2020.